THE UTILITY OF LOW COST THERMAL SENSORS IN ARCHAEOLOGICAL RESEARCH

Bryan S. Haley
Jay K. Johnson
Richard Stallings

Report Prepared for the Office of Naval Research
NASA Grant NAG5-7671

Center for Archaeological Research
University of Mississippi
December 2002

INTRODUCTION

The utility of airborne remote sensing techniques in archaeological research has been explored in a number of projects since the early 1970s. Thermal prospecting particularly has shown some promise for detecting subtle archaeological features. Thermal sensors have the potential to detect buried shallow archaeological features over a large area. In the southeastern United States, this task is made more difficult by the subtle nature of the features and the ground cover. Indeed, prehistoric sites in the southeast U. S. would rank among the more challenging settings for remote sensing. In addition, thermal sensors have traditionally been impractical because they were expensive and lacked scheduling flexibility. Newer, low-cost, thermal sensors may reduce these problems and allow archaeologists to maximize their potential. The following report explores the utility of an Agema 550 thermal infrared camera in the detection of features on a large, late prehistoric, southeastern site.

THEORETICAL SUMMARY

Archaeological features may be detectable with thermal prospecting if physical properties of the feature differ enough to cause a contrast that is visible in an image. The thermal contrast of an archaeological feature is determined by several physical properties of the targeted materials, including thermal conductivity (k), volumetric specific heat (Cv), and the thermal diffusivity (Γ) (Perisset and Tabbagh 1981:170). These can be used to calculate thermal inertia (P), which is perhaps a more convenient property to explain the thermal behavior of subsurface archaeological targets. Thermal inertia is expressed by

$$P = k / (\Gamma) = \sqrt{(k\ Cv)}.$$

Because thermal properties of subsurface targets are difficult to measure, this equation may not be of practical use for archaeologists. However, it is conceptually useful since thermal inertia is inversely proportional to the response of the ground to thermal radiation. In an archaeological setting, this is largely determined by soil moisture and particle size. For example, an archaeological feature that collects soil moisture will have a higher thermal inertia than the surrounding soil matrix. Thus, it would heat and cool relatively slow, causing it to show less temperature fluctuation through the diurnal cycle (Figure 1).

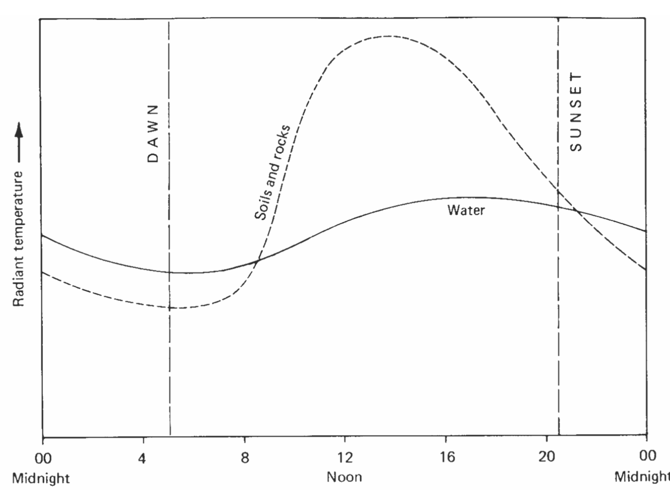

Figure 1. Diurnal variation in temperatures of soils and rocks compared to water (Lillesand and Kiefer 1994).

In order to reveal archaeological features, the diurnal heating cycle must therefore be considered. In the morning, as the sun heats the ground, a subsurface feature may be detected as a positive or negative anomaly. For example, a buried pit feature that traps moisture will result in a negative anomaly in the morning. This results because moisture effectively increases the thermal inertia of the pit feature. In the evening, this situation would be reversed since the thermal gradient would be from the ground towards the atmosphere.

Some research (Perisset and Tabbagh 1981) has been conducted in revealing archaeological features with long-term heat flux variation. This has the potential to reveal deeper features than with diurnal variation. However, this requires measurement of soil temperatures and other quantities over long periods time, which is less practical. Therefore, this method appears to have less potential for archaeological survey.

PREVIOUS RESEARCH

A number of projects have been conducted that focus on the use of thermal sensors for archaeological prospecting. These cover a wide range of archaeological targets, but are primarily over rather large and substantial features. In addition, most of the projects have focused on the use of very expensive sensors, such as those operated by NASA. The following is a brief description of some of the major literature.

An early application of thermal scanners was Berlin's (1975, Berlin et al. 1977) use of detection of a prehistoric agriculture system in the Southwest. A broad-range thermal radiometer, sensitive from 8 μm to 14 μm, was used to generate thermograms for an area of Arizona in April 1966. Anomalies in the imagery were interpreted as prehistoric agricultural plots. They were not visible on black and white aerial photographs. The agricultural plots were made up of a series ridges and swales. Ridges were capped by a layer of basaltic ash, while the swales large exposed buff soil areas. A 24 hours temperature history revealed the higher thermal diffusivity of the ridges caused them to heat faster than swales. Maximum temperature differences were between 1.1 degrees to 6.2 degrees. Based on nearby excavations, the features were found to be of Sinagua origin, dating from about 1150 A.D.

Perisset and Tabbagh (1981, see also Scollar et al. 1990) demonstrate the use of thermal prospection in archaeological applications and provide one of the most technical accounts of the physics involved in such research. Here, determining times of maximum anomaly contrast, subsurface features at some depth are detected. Examples given consist of several Neolithic camps, necropolises in France, and ancient roads and fields. A discussion of physical quantities is included, including the importance of heat flux, conductivity, thermal diffusivity, volumetric heat, and thermal inertia. By measuring these properties for a superficial layer, an anomaly, and the surrounding soil matrix, contrast coefficients are determined to how visible archaeological features will be in thermal imagery. Results show the authors were successful in determining the best times for acquisition of thermal imagery. One problem cited by the authors, and illustrated by their work, is that interpretation is more complicated than other types of prospection, such as magnetometry. While this is undoubtedly true, advances in processing and equipment in the twenty years since this article was written have somewhat remedied this situation. The work is of theoretical importance for thermal remote sensing, but the quantities mentioned are often too difficult to measure to be practical.

Sever (1985) and Gibson (1987) describe and effort to use the Thermal Infrared Multispectral Sensor (TIMS) at the late archaic period Poverty Point site in eastern Louisiana. TIMS acquires six narrow bands of data covering the thermal infrared portion of the electromagnetic spectrum and is capable of discerning differences in temperature of .3 °C or less. At the altitude flown, the ground resolution of the imagery was 5 meters. Based on later ground truth excavation, anomalies in the thermal data were caused by barrow pits, fill episodes, a ramp, and a corridor. In addition, several areas of the site's concentric rings were highlighted. However, several other anomalies were later determined to be of historic origin. Another problem with this research is that a detailed account is unavailable.

Sever has also applied the TIMS sensor to the detection of roads and subsurface features in Chaco Canyon in the American southwest. This work is described in Sever and Wiseman (1985), and Sever and Wagner (1991). From the TIMS imagery, a number of Anasazi roadway sections, invisible both from the ground and in color infrared photography, were identified. Also, subterranean walls, agricultural fields, and the location of several sites were determined. Image processing techniques in the form of high pass Gaussian filters were used to enhance the data. Several potential factors, including disturbances in soil texture, changes in microtopography, and changes in soil moisture, are cited as producing features visible in the TIMS imagery.

One example of low-cost thermal prospecting in archaeology is presented by Ben-Dor et al. (1999), who successfully used a thermal scanner to reveal features at the Early Broze Age site of Tel Leviah, located in the Golan Heights region of Israel. An Inframetrics Model 760 thermal radiometer, which is sensitive from 3 μm to 12 μm, was flown over the site aboard a helicopter. Imagery was acquired in the early morning, when it was determined that the thermal gradient between the buried walls and the soil above would be greatest. A limited amount of excavations had revealed that structures at the site were composed of basalt and covered by a layer of soil ranging from 5 cm to 50 cm in thickness. Image processing was performed in ENVI and consisted of georeferencing the thermal imagery to black and white aerial photography. Lineaments were revealed that seemed to correspond in form and orientation to buried structures. The successful delineation of the features was related to dramatic differences between the thermal properties of the basalt and the surrounding soil matrix.

Previous research at the Hollywood site (Johnson et al 2000, Haley 2002) analyzed a wide variety of airborne remote sensing systems, including the thermal infrared bands of the Advanced Terrestrial Land Applications Sensor (ATLAS). ATLAS is a 15 band sensor that includes 6 bands in the thermal infrared range, essentially duplicating the spectral capabilities of the TIMS sensor. ATLAS is operated by NASA and usually flown aboard a Learjet. Three sorties were flown over Hollywood, one in the morning, one at midday, and one just after sunset. The resultant 2.5 meter imagery was georeferenced to the Hollywood site grid system and processed using Erdas Imagine 8.4 software. By enhancing the contrast in the morning image, several interesting thermal anomalies were revealed. Several mound remnants were visible as relatively cool elliptical patterns. Excavation revealed that the mounds, which had been leveled by modern agricultural activities, were composed of fill that contrasted with the surrounding soil matrix, which itself had been artificially built up around them. Also, the area to the south of the largest mound and inside the outer mounds exhibited relatively high thermal readings. Excavation revealed this area was an artificially raised plaza. Despite these successes, little was revealed about buried structures at the site in the thermal bands. Also, ATLAS imagery is expensive and this would limit its potential to archaeologists.

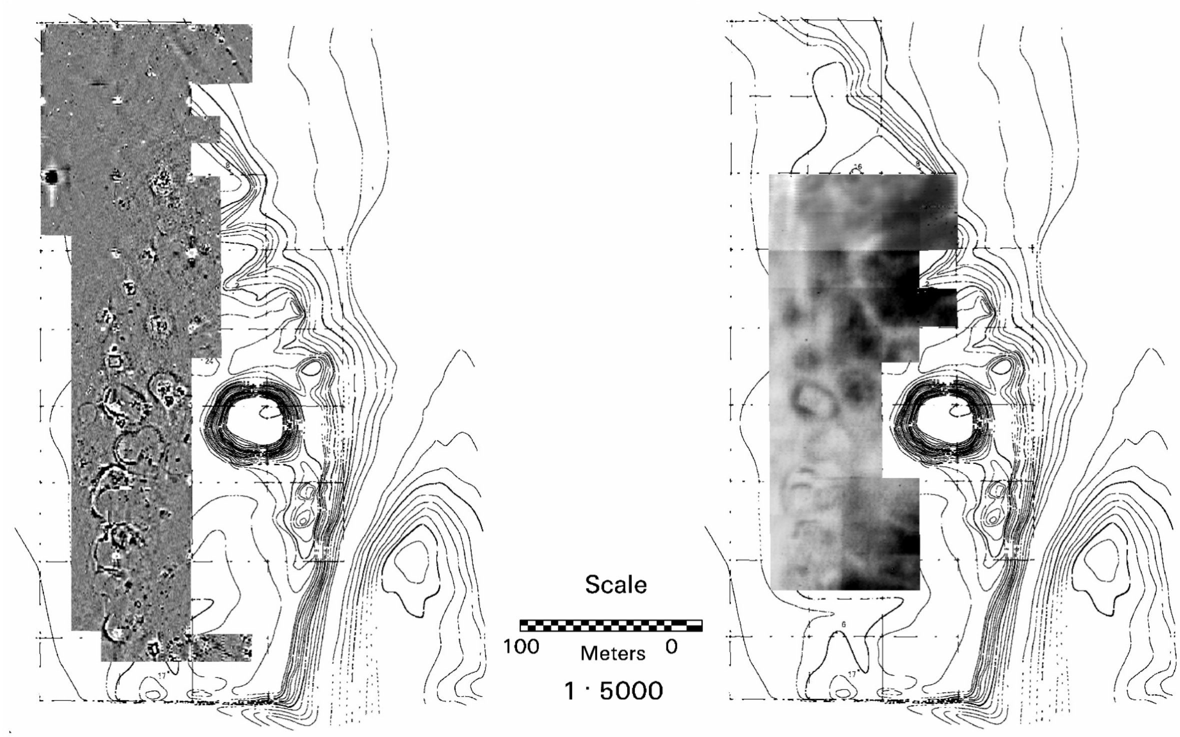

Figure 2. Results from Clay's 1998 earth conductivity (left) and fluxgate gradiometer (right) survey with topographic map in the background (from Johnson et al 2000).

PREVIOUS RESEARCH AT HOLLYWOOD MOUNDS, TUNICA COUNTY, MISSISSIPPI

The Hollywood site (15TU500) is located in Tunica County, Mississippi a few miles east of the current channel of the Mississippi River. It is located in the Yazoo Basin and within a larger region called the Delta, which was formed by meander episodes of the Mississippi River. As a result of this process, the soil in the region is low lying and fertile (Johnson et al. 2000:3). Hollywood Brake, an abandoned channel of the Mississippi River, is located just to the east of the site. This channel most likely formed an oxbow lake during the time Hollywood was occupied.

The site is located on a natural levee formed by the action of this channel (Johnson et al. 2000:3). Today, the channel scar, located to the east of the site, is composed of clays. The eastern boundary of the levee is marked by an abrupt change to courser-grained sands, which become gradually finer grained in a westerly direction. Eventually the levee subsides to the west of the site and finer-grained clays are again encountered.

Hollywood belongs to a cultural tradition known as Mississippian. Mississippian people lived throughout much of the southeastern United States from 900 until European contact, built large platform mounds, were organized politically into chiefdoms, relied on corn agriculture, and made shell tempered pottery. Hollywood was a sizable Mississippian period mound center that, based on ceramic and radiocarbon evidence, was occupied from 1300 to 1450 A.D., although it may have been used as ceremonial center at other times. The amount of mound construction at the site indicates significant status differences existed among the population of the region. Typically, Mississippian mounds supported houses or ceremonial structures associated with elites. Clearly, Hollywood was important in the regional social system of the Late Prehistoric Delta region.

A project was begun in May of 1997 designed to test an array of remote sensing techniques at Hollywood. As part of the remote sensing activities of the research, Dr. R. Berle

Clay of Cultural Resource Analysts of Lexington, Kentucky conducted a geophysical survey of the site. This included fluxgate gradiometer, which is a specialized type of magnetometer that measures the magnetic gradient by employing two sensors placed in a vertical configuration. An earth conductivity instrument, which primarily responds to differences in the moisture ion content of soils, was also used by Clay. Over several visits, the majority of the area of the site was surveyed. The resultant imagery (figure 2) shows a number of clear house patterns, which are rectangular in shape and 8 meters to 10 meters across. The imagery also reveals ellipses of daub, which is a brick-like substance that was produced when Mississippian people burned their house to clear for new construction. Limited test excavation has indicated that the elliptical patterns were produced when the daub was pushed down the side of the substructure mounds. These are the same patterns that were visible with the thermal bands of the ATLAS sensor.

RESEARCH DESIGN

To test the utility of low-cost thermal infrared sensors at the Hollywood site, an Agema 570 camera was acquired. The Agema 570 is a broadband thermal infrared camera manufactured by Flir Systems Incorporated. The Agema looks much like a standard video camera (figure 3). However, it is a precision digital thermal radiometer capable of measuring differences of temperature to .2 degrees Celsius (FLIR Systems 1996:8-1). The camera is sensitive to radiation with wavelengths of 7.5 mm to 13 μm, covering the upper region of the thermal infrared portion of the electromagnetic spectrum. A cutoff at 7.5 mm avoids atmospheric interference below this range. The camera has a 24 by 18 degree lens and produces a digital image composed of 320 by 240 pixels with a Focal Plane Array detector (FLIR Systems 1996:8-1). This equates to a field of view of 42 by 32 meters and a spatial resolution of about 13 centimeters at 100 meters altitude (FLIR Systems 1996:8-3).

When used by hand, the instrument is controlled by a series of buttons on the top and back of the unit. The user can focus, equalize the contrast, and freeze from this panel. Real time thermal measurements are shown through an eyepiece on a color LCD display. Various color schemes can be assigned to the thermal imagery that is displayed. Images can then be saved onto a flash card contained within the camera. Approximately 700 thermal images can be saved on the standard 170-megabyte card.

Figure 3. Agema 570 thermal infrared camera.

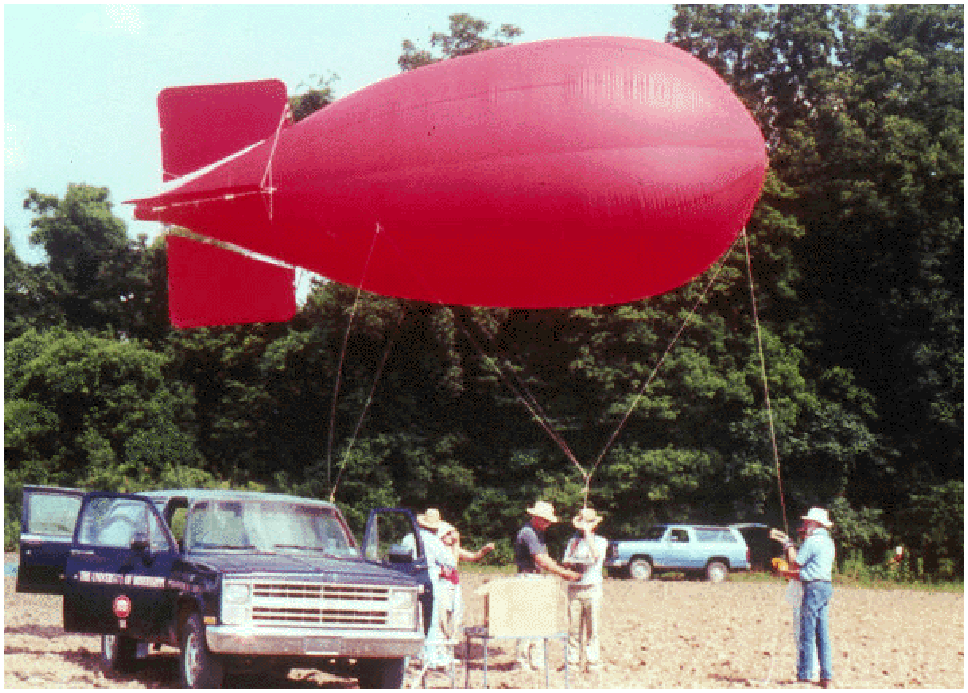

Figure 4. Helium blimp owned by the University of Mississippi.

For remote acquisition, a 25 foot, tethered, helium blimp was acquired (figure 4). A wireless link allows the camera to be controlled from a laptop computer on the ground. Real time video is transmitted to a video monitor on the ground. Thus, when an appropriate scene is in view in the monitor, the image can be saved on to the flash card carried onboard the camera. The blimp is usually flown at an altitude of 100 to 150 meters.

Proprietary software produced by FLIR, called IRwin, is used to extract the data from the flashcard. IRwin can be used to display the imagery with several color palettes and adjust the temperature range. It can also be used to output an image to a .BMP file. The .BMP images can then be imported into image processing software, such as ERDAS Imagine, for further analysis.

Three house patterns and one mound remnant were imaged with the Agema to test the utility of the Agema sensor (Figure 5). House 1 is centered at S193/E134 and is situated on an elevated area of the levee sands on the eastern edge of the site. House 2, centered at S197/E78, is located slightly off the levee sands on a slight down slope. House 3, centered at S193/E45, is well back from the levee sands on a slightly lower area of tighter soils. The mound remnant is located to the west of the largest mound and is one of the more apparent

Four field trips were made between July and December in order to collect data over these targets. Field notes provided relative humidity and temperature during the data acquisition periods. In order to determine the effects of moisture on the thermal sensing, rainfall data was acquired from the National Climatic Data Center. The nearest rain station data available were recorded at Arkabutla dam, a distance of approximately 25 kilometers to the east of the test site. In addition, sunrise and sunset times were acquired to determine the effect of the diurnal heating cycle.

Thermal data was georeferenced to the Hollywood site grid system to allow accurate comparison with other data. Fluxgate gradiometer data, which clearly shows the four targeted features, was used to evaluate the thermal data. Imagery was compared using ERDAS Imagine 8.5 software. The results for each acquisition date are described below.

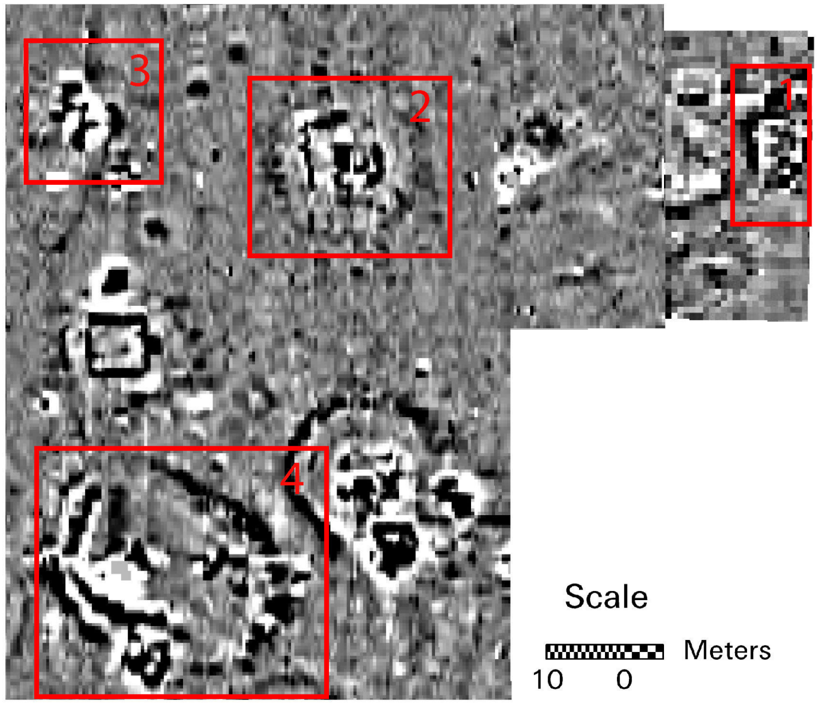

Figure 5. Gradiometer image showing targeted features from the Hollywood site. Features 1 – 3 are buried houses and feature 4 is a mound remnant.

RESULTS

July 21, 1999

The first date of image acquisition, July 21, occurred 11 days after an episode of rainfall (figure 6). Although there was a rainfall of about 1.75 inches on July 10, it is likely that a good deal of drying took place by July 21. Temperatures and relative humidity measurements (table 1) show that the weather was very hot and humid, typical for July in Mississippi. The temperature variation between 12:44 and 23:52 on that day was about 20 $^{\circ}$F.

Thermal data was acquired on July 21 for nearly 12 hours from 12:38 to 12:13. Sunrise for this day was about 6:07 and sunset was at 20:06, which means midday occurred at about 13:06. This is the time of the most intense thermal radiation from the sun. Ground targets should begin to cool after midday and cool dramatically at sundown.

The first set of the July 21 images were acquired at 12:44, 14:23, 14:41, and 15:48. Among the house targets, House 1 is the clearest (figure 7). It is visible as a cooler area on the eastern half of the image. The maximum temperature difference between the anomaly and the ground surrounding it is 3 $^{\circ}$C. House 2 may be visible as a slightly warmer area, but is not very apparent, and House 3 is not visible at all. There is variation within the mound remnant, but it does not seem to correspond to the geophysical data sets. An anomaly with a maximum of 3 $^{\circ}$C surrounds a large plastic PVC pipe used as a grid marker.

The 12:44 timing would place the House 1 image just before solar noon. Since the anomaly is cooler than the surrounding soil, it must have a higher thermal inertia. This is probably caused by a higher level of moisture associated with the feature. Interestingly, House 2, House 3, and the mound remnant are not particularly visible in the imagery. The reason for this is probably related to differences in the texture of the soil surrounding the features. House 1 is the only target found within the levee sands at the eastern side of the site. Also, House 2, House

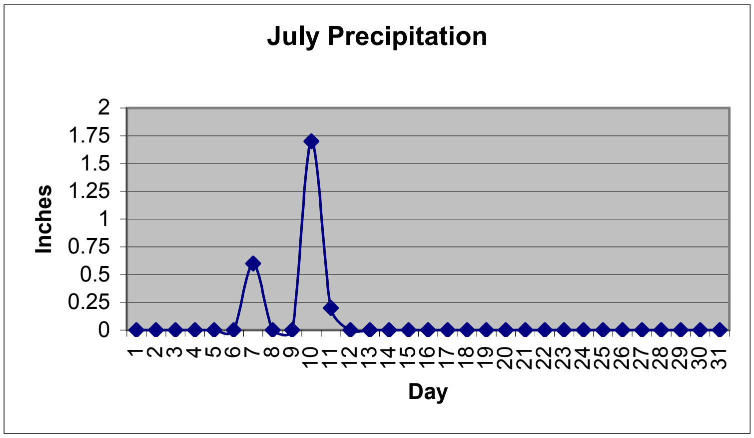

Figure 6. Precipitation for July 1999.

Time	Temperature (^{O}F)	Relative Humidity (%)
12:44	95.5	60
21:06	82.5	75
23:52	75.3	86

Table 1. Temperature and humidity data for July 21, 1999.

3, and the mound remnant were acquired several hours after the House 1 image and several hours after solar noon. Often, a thermal crossover takes place at this time, which would reduce the contrast between the features and the surrounding soil.

The next set of imagery was acquired after sunset, starting at 20:59. In these images, House 3 and House 2 are visible as relatively cool anomalies. House 1 and the mound remnant are not visible in this set of images. Because these images were certainly acquired after the afternoon thermal crossover, the visibility of House 3 and House 2 suggest they have lower thermal inertia values than their surrounding matrices. Thus, they are cooling relatively fast. This contrasts with the earlier result for House 1, probably due to differences in the physical properties of the surrounding soils. House 1 is no longer visible after sunset because the temperature of the feature and the soil has stabilized.

The final set of images was acquired several hours after sunset. Results were similar to the previous set. Houses 2 and 3 were, once again, visible, although the difference between the anomaly and the surrounding soil was slightly less dramatic. House 1 and the mound remnant are still not visible.

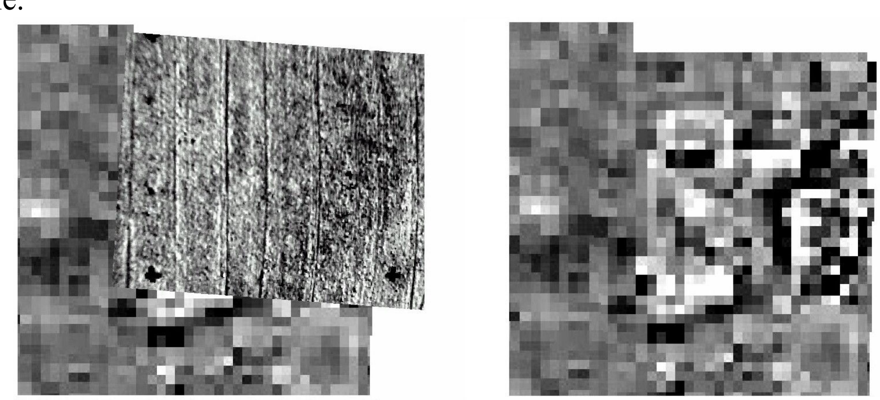

Figure 7. 12:44 Agema thermal image layered over gradiometer data (left) and gradiometer data (right).

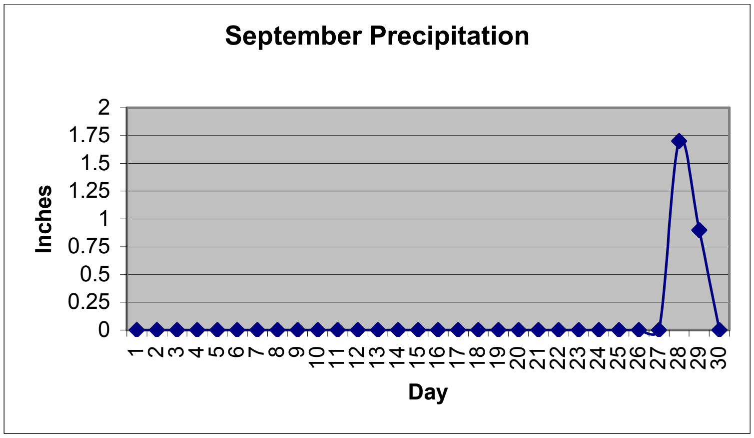

Figure 8. Precipitation for September, 1999.

Time	Temperature (°F)	Relative Humdity (%)
15:12	86	20
19:57	69.8	70
20:42	54	89

Table 2. Temperature and humidity data for September 30, 1999.

September 30, 1999

The data acquired on September 30, 1999 took place at the end of a rainfall episode. Approximately 1.75 inches of rainfall fell on September 28, followed by about .9 inches the following day (Figure 8). The ground would have contained some of this moisture on September 30. Temperature and humidity levels are shown in table 2. A variation of 31 °F was measured between 15:12 and 20:42. Thus, although it was cooler overall, there was more thermal variation than on during the July 21 images.

Images were acquired beginning at 15:12 until 21:59. Records show that sunrise occurred on 6:54, sunset at 18:48, and midday was 12:51 for this date. The beginning time of image acquisition, therefore, may have been slightly before the time of the afternoon thermal crossover.

In the first set of images, acquired from 15:21 to 15:26, the four features are not visible. Instead, variation seems to primarily be related to surface soil features such as plow marks, which exhibits a maximum of about 3 °C variation in temperature. This result is expected since the proximity of acquisition time to thermal crossover would limit the thermal contrast of subsurface features. Variation is confined to near to shallow features at this time because they respond more quickly to thermal radiation changes.

The second set of images was acquired just after sunset. These do not show the surface variation problem experienced with the earlier set. As with the July 21 images acquired after sunset, Houses 2 and 3 are visible as cool anomalies. House 1 is not visible in the set, although there is a good deal of variation. Thermal anomalies in the mound remnant somewhat correspond to features in the gradiometer imagery. However, it is difficult to say for certain whether the archaeological feature caused these.

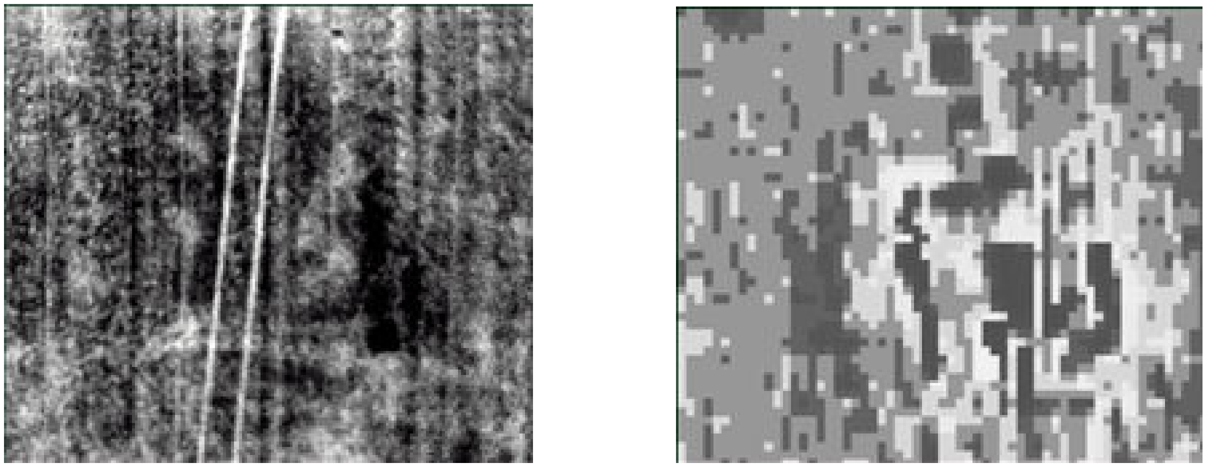

Figure 9. Nighttime thermal image of House 2 (left) and gradiometer image (right).

The final set of imagery from September 30 started at 22:42. Results are similar to the previous set, showing that the temperature trajectory somewhat stabilizes after sunset. Eventually, of course, the temperatures would approach the same value, however. An image of House 2, is particularly clear in this set of images, especially when compared to gradiometer data of the same area (figure 9).

October 5, 1999

October 5 was preceded by 5 days of dry weather that following the rain episode at the end of September (figure 10). Temperature and relative humidity for acquisition times is shown in table 3. There was a temperature difference of about 30 $^{\circ}$F between the first and last images.

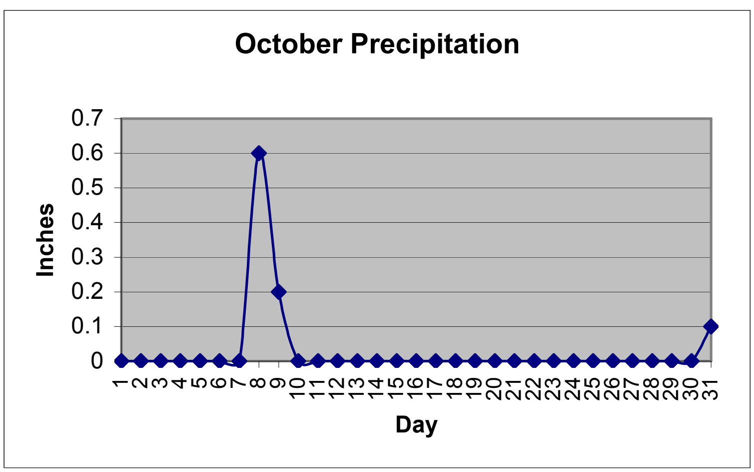

Figure 10. Precipitation for October, 1999.

Time	Temperature ($^{\circ}$F)	Relative Humdity (%)
16:44	80	24
19:07	67.3	37
21:55	55	65

Table 3. Temperature and humidity data for October 5, 1999.

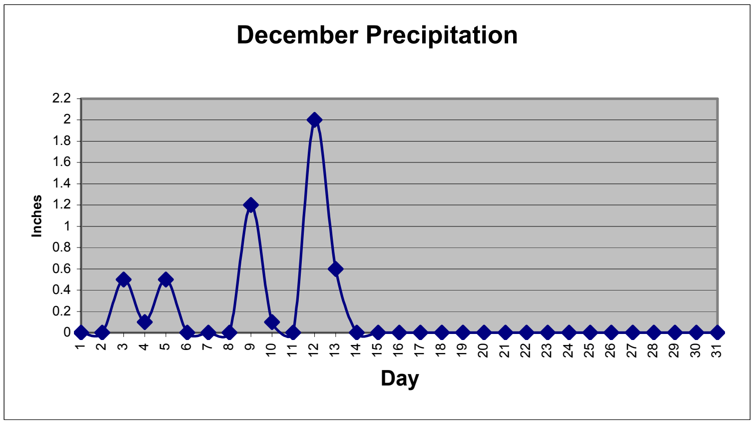

Figure 11. Precipitation for December 1999.

Time	Temperature (°F)	Relative Humdity (%)
5:33	54.5	71

Table 4. Temperature and humidity data for December 8, 1999.

Images were acquired on October 5 from 16:44 P.M. to 21:59. Sunrise occurred at 6:57 that day with sunset at 18:41 and midday at 12:49. Thus the time of beginning time of 16:44 may be near the time of thermal crossover on this date.

Like the earlier images from September 30, 4 images acquired from 16:44 to 16:55 were not successful at showing archaeological features. Variation, once again, seems confined to surface features.

Images acquired at 19:07 and 19:55 of House 1 and the mound remnant were not successful in revealing the prehistoric features. Variation occurred, but did not correspond to any anomaly in the gradiometer image or any known archaeological source.

Another set of images was acquired about 3 hours later. The only feature definitely visible in the imagery is House 3, which shows a maximum temperature variation of 1 °C to 2 °C. There is an anomaly that may also be associated with House 2, but its location is somewhat transposed. However, double checking the georeferencing revealed no errors. House 1 and the mound remnant are not visible.

Overall, the October data sets are less successful than the two previous ones. This is interesting considering it is only slightly cooler than the September date. The temperature range, in fact, is greater than the July date and only slightly less than the September date. Also, the proximity to rainfall episodes falls between the amounts for the July and September dates. There must be some other explanation, although based on the study variables presented here, none can be offered.

December 8, 1999

There were three small rainfall episodes just before December 8, when images were acquired over a period of 1.5 hours in the evening (figure 11). These took place on December 3, 4, and 5. On December 6 and 7, there was no rain. This recent rainfall might affect the ground moisture level for December 8.

Two sets of December 8 images were recorded from 17:33 to 18:57. Sunrise occurred at 6:49, sunset occurred at 16:56, and solar noon occurred at 11:53. Therefore the data sets were

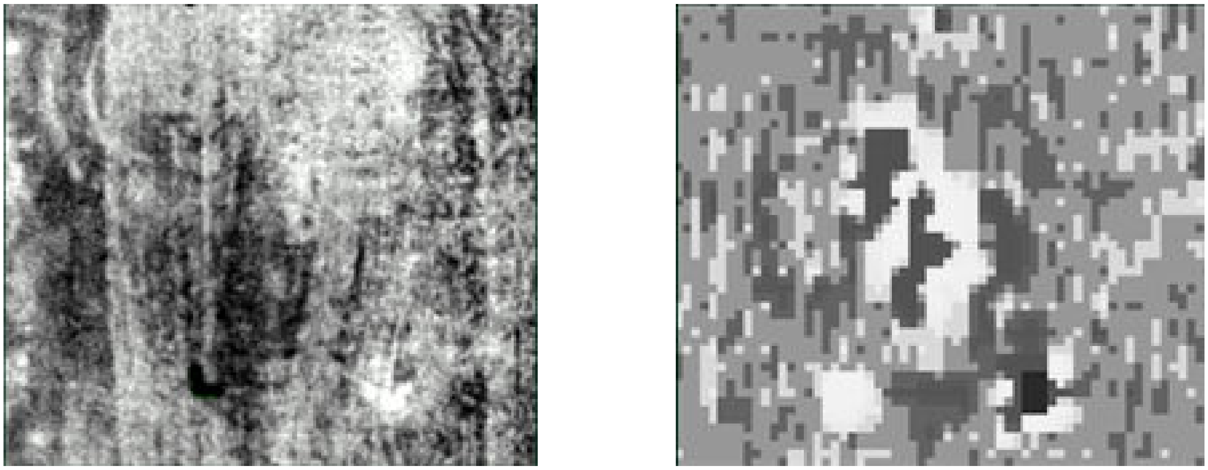

Figure 12. House 3 in thermal data (left) and gradiometer data (right).

recorded after the sun had set. Overall, diurnal temperature variation is less at this time than during the summer or fall months and it was relatively cool (table 4).

The first set of images is fairly noisy. There were significant anomalies, but none corresponded to features in the geophysical data. A 17:36 image covering House 3 is the only one that seems to show a known feature (figure 12). The thermal anomaly has maximum temperature difference of about 2 °C to 3 °C.

The second set of images was similar to the first. Only House 3 is apparent in these images, again with a maximum temperature variation of about 2 °C to 3 °C. In fact, this is one of the clearest of the images of House 3. There are many anomalies that approach this magnitude in the other images that do not correspond to features in the other imagery.

This date is perhaps the least effective for revealing archaeological features in the imagery. Moreover, the significant nonarchaeological variation in almost all images could be problematic. If only this date were used to map features at the site, the result would be completely incorrect.

DISCUSSION

The results of the thermal imaging are shown in Table 5. In some cases, the technique worked quite well and the resultant anomaly could be explained in terms of the thermal inertia differences of the materials imaged. It had been thought that house floors would exhibit enhanced moisture retention due to compaction and the remaining structural material. Water molecules have a high thermal inertia and would, in general, show more uniform temperatures throughout the diurnal cycle. That is, they would be relatively cool some time after the sun begins to heat the ground up and relatively hot after sun intensity lessens and the ground cools.

Imagery of House 1 supports this hypothesis. The feature is visible as a cool anomaly at 12:44 on July 21. The feature is heating slower than the surrounding soil and must have a higher thermal inertia. Sandy soil, which surrounds it, has a lower thermal inertia, providing the necessary contrast.

However, House 1 is only visible in one image. All other data sets were acquired beginning later in the day. A plot of the temperatures of the feature and the surrounding neutral soil, measured in the same location on three images, shows the problem (figure 13). There is insufficient contrast between the feature and the soil to allow it to be visible after the first

Time	Feature	Feature Visible	Days After Rain	Soil Texture	Anomaly Variation
July 21					
12:44	House 1	Yes	10	Sand	Cool
14:23	House 2	?	10	Clay / Sand	Warm?
14:41	House 3	No	10	Clay	
15:48	Mound Remnant	No	10	Clay	
20:59	Mound Remnant	No	10	Clay	
21:06	House 3	Yes	10	Clay	Cool
21:11	House 2	Yes	10	Clay / Sand	Cool
21:18	House 1	No	10	Sand	
23:52	House 1	No	10	Sand	
23:59	House 2	Yes	10	Clay / Sand	Cool
September 30					
15:12	House 1	No	1	Sand	
15:21	House 2 / 3	No	1	Clay / Sand	
15:21	House 2	No	1	Clay	
15:26	Mound Remnant	No	1	Clay / Sand	
19:57	Mound Remnant	?	1	Clay	Cool?
20:10	House 3	Yes	1	Clay	Cool
20:11	House 2 / 3	Yes / Yes	1	Clay / Sand	
22:17	House 1	No	1	Sand	
20:42	House 1	No	1	Sand	
22:51	House 2	Yes	1	Clay / Sand	Cool
22:52	House 3	Yes	1	Clay	Cool
23:00	Mound Remnant	?	1	Clay	Cool?
October 5					
16:44	House 1	No	5	Clay	
16:49	House 2	No	5	Clay	
16:53	House 3	No	5	Clay / Sand	
16:55	Mound Remnant	No	5	Sand	
19:07	House 1	No	5	Sand	
19:56	Mound Remnant	No	5	Clay	
21:55	House 1	No	5	Sand	
21:57	House 2 / 3	? / Yes	5	Clay / Sand	Cool
21:59	Mound Remnant	No	5	Clay	
December 8					
17:33	Mound Remnant	No	3	Clay	
17:36	House 3	No	3	Clay	
17:38	House 2	No	3	Clay / Sand	
17:44	House 1	No	3	Sand	
18:51	Mound Remnant	No	3	Clay	
18:53	House 1	Yes	3	Clay	Cool
18:55	House 2	No	3	Clay / Sand	

Table 5. Summary of thermal imaging results.

measurement. The late timing of the thermal crossover, near midnight, suggests both materials have relatively low thermal inertia values.

The other two houses are much more consistent in the imagery because most of the images were acquired later in the day, where they are visible as regions of low thermal response. The thermal curves for the two features (figure 14, figure 15) confirm that the features are opposite thermal from House 1. This would suggest that the features had a higher thermal inertia than the surrounding matrix, which caused it to cool more rapidly. This contradicts the earlier hypothesis and suggests house remnants can also enhance drying in certain soil types. Clearly, the thermal and moisture characteristics of buried prehistoric structures vary widely.

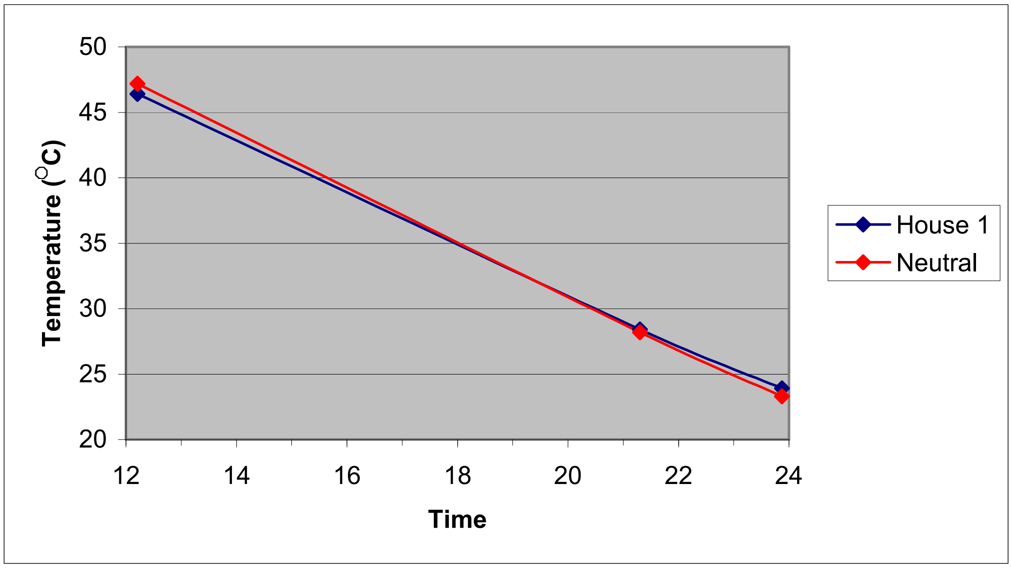

Figure 13. July 21 thermal curve for House 1.

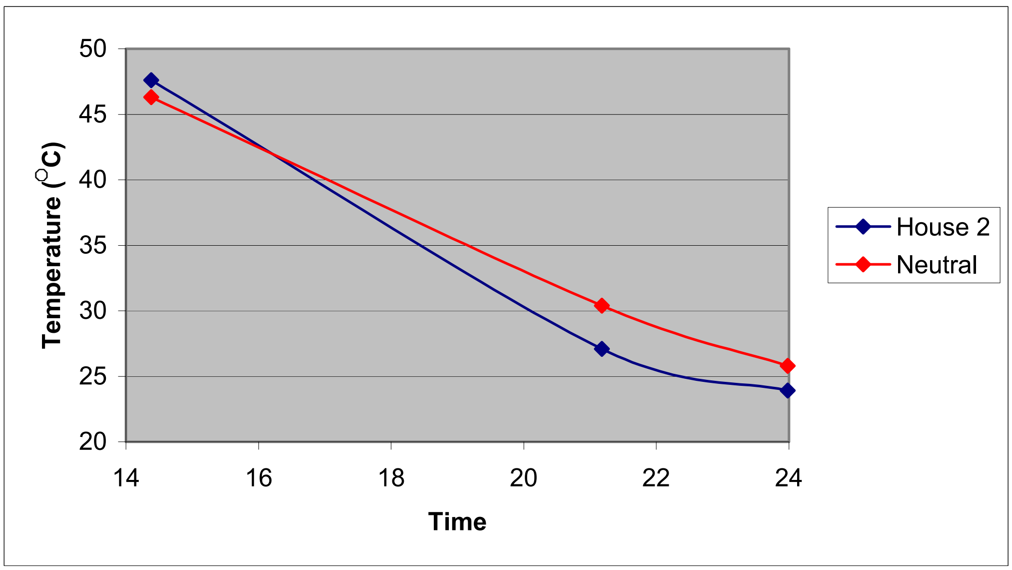

Figure 14. July 21 thermal curve for House 2.

Soil texture variation was probably responsible for the variable thermal behavior of the house targets. House 1, which is located along the levee sands at the eastern edge of the site, reacted very differently than House 2 and House 3, which are situated on the fine grained soils away from the levee. Moreover, House 3 and House 2 differ slightly because soils become progressively more clayey to the west.

Topography may have also affected the moisture associated with the features. The area containing the houses varied in elevation by about 1.6 meters. House 1 is located at the crest of the natural levee of an extinct channel of the Mississippi River, House 3 is positioned on the back slope of the levee, and House 2 is intermediate. Higher elevation might be expected to drain better than lower elevations. In this case, topography mirrors the hypothesized affect of soil texture. Thus, it is difficult to tell how much of a role each plays.

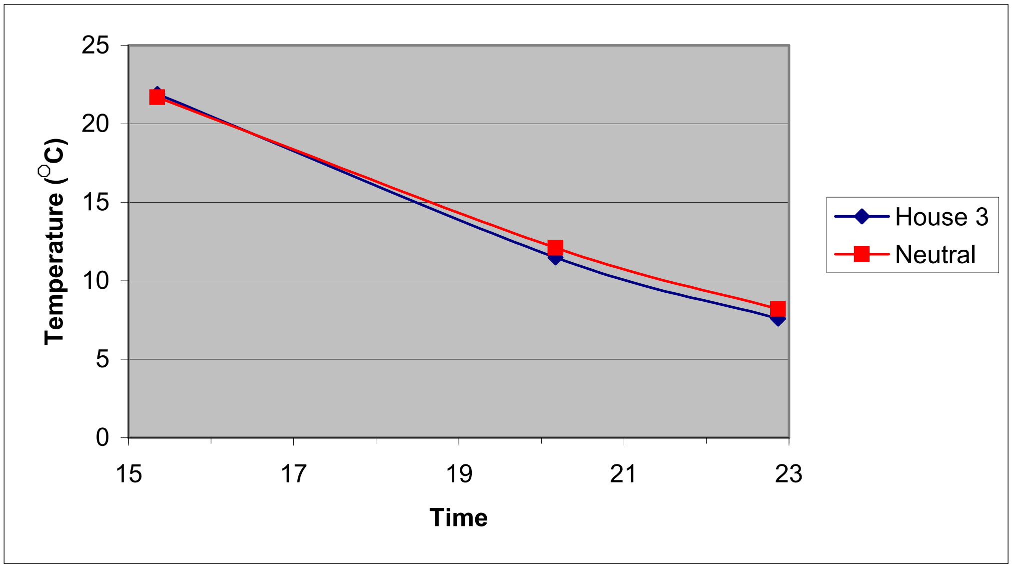

Figure 15. September 30 thermal curve for House 3.

However, the results presented in the previous section suggest that predicting the thermal behavior of archaeological features is complex. The study variables, which were chosen because they should have an impact on thermal behavior, were not always sufficient to explain the observed phenomena.

Rainfall data was not found to correspond with the results of the thermal data. In fact, the best dates for thermal data, July 21 and September 30, were the most variant in terms of proximity to rainfall episodes. October 5 and December 8 dates produced less successful data, but proximity to rainfall episodes fell within the range for the two other dates.

Temperature also did not always have the expected effect on the thermal data. For example, a relatively large range of temperature for the day did not always produce the best data. The July 21, which produced good thermal data, showed a temperature variation of just over 20 °F from 12:44 to 23:52. For the October 5 acquisition date, however, a 25 °F temperature difference was experienced. Imagery acquired on this date was of much less successful in revealing the archaeological features. One might expect, then, that sun intensity was a factor in the success of the imagery. The July sun is much more intense than in October because of the angle. However, the September imagery, acquired only 6 days before the October 5 imagery, was nearly as good as the July imagery. Other factors that were not recorded, such as cloud cover, were likely responsible for these results.

The utility of thermal infrared sensors may be best evaluated by comparing it to sensor systems that are more routinely used in archaeological survey. Primarily, these consist of near-surface geophysical sensors, such as magnetometry, electrical resistivity, earth conductivity, and ground penetrating radar. The ability of these sensors to quickly survey large areas is well established (Clark 1990, Bevan 1998). Several states, in fact, have encouraged their use in cultural resource management archaeology by including them in state guidelines (Georgia Council of Professional Archaeologists 2001).

Geophysical techniques offer several advantages over thermal sensors. For the site studied in this project, for example, magnetic gradient survey was, in most ways, much more productive than the thermal sensing. The level of detail is so high that features such as hearths, wall trenches, and entrances are sometimes visible. However, these results are among the best that one can expect from geophysical survey on an archaeological site. Also, they vary considerably with the instrument used.

Geophysical survey may be less limited by weather conditions, particularly related to rainfall, than thermal sensing. For example, magnetic gradient survey is almost completely unaffected by ground moisture changes. However, other remote sensing techniques, such as earth conductivity, electrical resistivity, and ground penetrating radar, are highly dependent on ground moisture levels. In some cases, a substantial amount of rain can render these instruments useless.

Finally, ground cover conditions are less of a concern with geophysical survey. Although this was not tested in this project, it is likely that successful thermal data sets require that the ground to be almost completely clear of vegetation and other objects. This is a substantial drawback because much of the land in the southeastern United States is covered by uneven vegetation.

One advantage for airborne systems over geophysical systems is the ability to cover large areas rapidly. Although ground based geophysics is fast compared to traditional archaeological excavation, it often cannot match airborne systems. However, although thermal infrared sensors have the potential to be used to collect data for large areas rapidly, the system evaluated in this research was hardly quicker than the magnetic gradient instrument. A data set that covers 20 meters by 20 meters of site area often takes about 15 minutes to acquire in a magnetic gradient survey. The Agema thermal camera mounted aboard the helium blimp typically was able to cover produce a scene slightly larger than 20 meter by 20 meters. Acquisition was slowed by wind, which made it difficult to cover the targeted area. An airborne platform capable of higher altitudes would lessen this problem, although the resultant lower ground resolution would have to be sufficient to still detect the features.

The mound remnant was never clearly imaged in the research. Based on excavations, however, there is a substantial soil texture difference associated with this feature. Also, they are visible in the thermal bands of the Atlas sensor. The small scene size of the Agema imagery may be responsible for this failure. Once again, this could be remedied by higher altitude flights.

Additional types of archaeological targets may prove to be easier to detect with thermal infrared. For example, historic targets are typically less subtle features that may produce more substantial thermal contrasts and may be made up more regular patterns than the prehistoric features targeted in this research.

CONCLUSIONS

Low cost thermal-infrared sensors can be successful employed to reveal buried archaeological features. However, as is illustrated in this research, there are many variables that must be considered to predict the success of the technique. In fact, because of the complexity of the interplay of these variables, it may be impossible to the model results of thermal sensing. As a result, it may not be possible to determine the best time to acquire thermal imagery for a given target. Thus, the success rates of thermal imagery may be somewhat unpredictable.

Therefore, at this stage in research, the use of low-cost thermal infrared sensor systems should be considered an experimental technology. As such, its use should be considered, if possible, in archaeological reconnaissance. As sensors continue to become more advanced and less expensive, their utility as a method for surveying large areas for archaeological resources will surely improve. Still, it seems unlikely that it will ever be as effective as several of the more common geophysical techniques in surveying for prehistoric cultural resources in the southern United States.

REFERENCES CITED

Ben-Dor, Eyal, Juval Portugali, Moshe Kochavi, Michal Shimoni, and Lipaz Vinitzjy
1999 Airborne Thermal Video Radiometry and Excavation Planning at Tel Leviah, Golan Heights, Israel. Journal of Field Archaeology 26:117-127

Berlin, G. L.
1977 Archaeological Field Patterns Revealed in North-Central Arizona by Aerial Thermography, Soil Chemistry, Pollen/Plant Analysis, and Archaeology. American Antiquity 42:588-600.

Berlin, G. Lennis, J. Richard Ambler, Richard H. Hevly, and Gerald G. Schaber
1975 Archaeological Field Patterns Revealed in North-Central Arizona by Aerial Thermography. Proceedings of the American Society of Photogrammetry, October 26:231-243. Falls Church, Virginia.

Bevan, Bruce
1998 *Geophysical Exploration for Archaeology: An Introduction to Geophysical Exploration*. Midwest Archaeological Center Special Report No. 1. National Park Service, Lincoln, Nebraska.

Clark, Anthony
1990 *Seeing Beneath the Soil, Prospecting Methods in Archaeology*. 2nd Ed. B. T. Batsford Ltd., London, England.

FLIR Systems
1996 Agema 570, Operating Manual. FLIR Systems, Danderyd, Sweden.

Georgia Council of Professional Archaeologists
2001 *Georgia Standards and Guidelines for Archaeological Surveys*. http://www.georgia-archaeology.org/GCPA/Georgia_standards.pdf.

Gibson, Jon L.
1987 The Ground Truth About Poverty Point: The Second Season, 1985. University of Southwest Louisiana Center for Archaeological Studies Report No. 7. University of Southwestern Louisiana, Lafayette, Louisiana.

Haley, Bryan S.
2002 *Airborne Remote Sensing, Image Processing, and Multisensor GIS Analysis at the Hollywood Site, A Large Late Mississippian Mound Center.* Unpublished Master's Thesis, Department of Sociology and Anthropology, University of Mississippi, University.

Johnson, Jay K., Richard Stallings, Nancy Ross-Stallings, R. Berle Clay, and V. Stephen Jones
2000 Remote Sensing and Ground Truthing at the Hollywood mounds Site in Tunica County, Mississippi. Center for Archaeological Research, University of Mississippi. Submitted to for the Mississippi Department of Archives and History, House Bill 1502, Grant Project

GS# 501-074. Copies available from Mississippi Department of Archives and History, Jackson, Mississippi.

Lillesand, Thomas M., and Ralph W. Kiefer
1983 Remote Sensing and Image Interpretation. 3rd Ed. John Wiley & Sons, New York, New York.

Perisset, M. C., and A. Tabbagh
1981 Interpretation of Thermal Prospection on Bare Soils. Archaeometry 23(2):169-187.

Sabins, F. F.
1997 Remote Sensing, Principles and Interpretation. New York, W. H. Freeman and Company.

Sever, Thomas L. and David W. Wagner
1991 Analysis of Prehistoric Roadways in Chaco Canyon Using Remotely Sensed Digital Data. In Ancient Road Networks and Settlement Hierarchies in the New World, edited by Charles D. Trombold, pp.42-65. Cambridge University Press, Cambridge.

Sever, Thomas, and James Wiseman
1985 Remote Sensing and Archaeology: Potential for the Future. Report on a Conference, March 1- 2, 1984, pp. 30-37. National Aeronautics and Space Administration, John C. Stennis Space Center, Mississippi.

Scollar, I., A. Tabbagh, A. Hesse, and I. Herzog
1990 Archaeological Prospecting and Remote Sensing: Topics in Remote Sensing 2. Cambridge University Press, Cambridge.

Tabbagh, Alain
1978 Thermal Infrared Prospection of the Lion en Beauce Township. Archaeo-Physika 10: 700-709.